Naturwissenschaften (2009) 96:111–122
DOI 10.1007/s00114-008-0461-1

ORIGINAL PAPER

Nacre and false nacre (foliated aragonite) in extant monoplacophorans (=Tryblidiida: Mollusca)

Antonio G. Checa · Joaquín Ramírez-Rico · Alicia González-Segura · Antonio Sánchez-Navas

Received: 7 February 2008 / Revised: 3 September 2008 / Accepted: 20 September 2008 / Published online: 9 October 2008
© Springer-Verlag 2008

Abstract Extant monoplacophorans (Tryblidiida, Mollusca) have traditionally been reported as having an internal nacreous layer, thus representing the ancestral molluscan condition. The examination of this layer in three species of Neopilinidae (*Rokopella euglypta*, *Veleropilina zografi*, and *Micropilina arntzi*) reveals that only *V. zografi* secretes an internal layer of true nacre, which occupies only part of the internal shell surface. The rest of the internal surface of *V. zografi* and the whole internal surfaces of the other two species examined are covered by a material consisting of lath-like, instead of brick-like, crystals, which are arranged into lamellae. In all cases examined, the crystallographic *c*-axis in this lamellar material is perpendicular to the surface of laths and the *a*-axis is parallel to their long dimension. The differences between taxa relate to the frequency of twins, which is much higher in *Micropilina*. In general, the material is well ordered, particularly towards the margin, where lamellae pile up at a small step size, which is most likely due to processes of crystal competition. Given its morphological resemblance to the foliated calcite of bivalves, we propose the name foliated aragonite for this previously undescribed biomaterial secreted by monoplacophorans. We conclude that the foliated aragonite probably lacks preformed interlamellar membranes and is therefore not a variant of nacre. A review of the existing literature reveals that previous reports of nacre in the group were instead of the aragonitic foliated layer and that our report of nacre in *V. zografi* is the first undisputed evidence of nacre in monoplacophorans. From the evolutionary viewpoint, the foliated aragonite could easily have been derived from nacre. Assuming that nacre represents the ancestral condition, as in other molluscan classes, it has been replaced by foliated aragonite along the tryblidiidan lineage, although the fossil record does not presently provide evidence as to when this replacement took place.

Keywords Monoplacophorans · Mollusca · Biomineralization · Microstructure · Nacre · Foliated aragonite · Evolution

Electronic supplementary material The online version of this article (doi:10.1007/s00114-008-0461-1) contains supplementary material, which is available to authorized users.

A. G. Checa (✉)
Departamento de Estratigrafía y Paleontología,
Facultad de Ciencias, Universidad de Granada,
Avenida Fuentenueva s/n,
18071 Granada, Spain
e-mail: acheca@ugr.es

J. Ramírez-Rico
Departamento de Física de la Materia Condensada,
Facultad de Física, Universidad de Sevilla,
Avenida Reina Mercedes s/n,
41012 Seville, Spain

A. González-Segura
Centro de Instrumentación Científica, Universidad de Granada,
Paseo del Profesor Juan Ossorio s/n,
18071 Granada, Spain

A. Sánchez-Navas
Departamento de Mineralogía y Petrología, Facultad de Ciencias,
Universidad de Granada,
Avenida Fuentenueva s/n,
18071 Granada, Spain

Introduction

Due to the scarcity of material, relatively few studies have been done on the shells of present-day monoplacophorans (which constitute the Order Tryblidiida of the Class Tergomya; Peel 1991). The shell structure of *Neopilina*

galatheae Lemche, 1957, was first briefly described by Lemche and Wingstrand (1959). Their study was followed by the more detailed accounts of Schmidt (1959), Erben et al. (1968), and Meenakshi et al. (1970) on the same and on congeneric species (*Neopilina ewingi*, *Neopilina bacescui*, *Neopilina bruuni*). The first reference to nacre in Tryblidiida is that of Schmidt (1959), who observed that the fractured internal layer of *Neopilina* was lamellar, brick wall like, and aragonitic (as the rest of the shell), thus apparently displaying the basic characteristics of nacre. This opinion was later shared by Erben et al. (1968), and, from then on, all subsequent authors have expressed little doubt that the "nacre" of monoplacophorans is a true nacre.

According to previous knowledge, the shells of *Neopilina*, *Laevipilina*, and *Vema* are prismatonacreous (Schmidt 1959; Erben et al. 1968; Urgorri et al. 2005; Warén and Gofas 1996), whereas in *Micropilina*, the outer shell layer was not prismatic (Cruz et al. 2003). Thus, it seems that the shell of monoplacophorans retained the ancestral condition found in many bivalves (palaeotaxodonts, palaeoheterodonts, pterioids, and many anomalodesmatans), most Vetigastropoda and *Nautilus*.

Interestingly, very little attention has been paid to the "nacreous" part of the monoplacophoran shell and very few descriptions and images can be found in the literature. Meenakshi et al. (1970) and Cruz et al. (2003) report how monoplacophoran "nacre" is terrace like. Meenakshi et al. (1970) recognized a brick wall structure as well as the existence of interlamellar and intercrystalline membranes, as in typical nacre. In fact, they compared the shells of several species of *Neopilina* to those of prismatonacreous bivalves. Chateigner et al. (2000) applied X-ray diffraction and concluded that the monoplacophoran nacre-like layer has a fiber texture, with the *c*-axis as fiber axis.

Despite the valuable data contained in the previous studies, they do not provide a general overview of how this particular "nacre" is organized in the different parts of the shell and what is its crystallographic arrangement.

The study of the so-called "nacre" of monoplacophorans is important in two main respects. First, the pattern of organization of nacre is a main theme in biomineralization (Addadi et al. 2006; Cartwright and Checa 2007). It is well known that nacre is arranged terrace like in bivalves and tower like in gastropods (e.g., Erben 1972; Wise 1970; Mutvei 1978; Nakahara 1991). The knowledge of how nacre is organized in other groups, such as cephalopods and monoplacophorans, is particularly relevant for biomineralization models. Second, the relationship of Tryblidiida to other molluscan classes is presently unknown and the unraveling of how their "nacre" is fabricated might provide insights into this central issue.

We have analyzed the internal shell layer of three species of monoplacophorans included in the family Neopilinidae. Our main goal is to characterize it both from the morphological and crystallographic viewpoints in order to compare it with the nacre secreted by other molluscan classes. The information obtained will be put into a general evolutionary framework.

Material and methods

Material

We have examined three empty shells of *Rokopella euglypta* (Dautzenberg and Fischer 1897) and two of *Veleropilina zografi* (Dautzenberg and Fischer 1896). Locality: Atlantis Bank, NO of "le Suroli", Seamount 2, DW 261, Coordinates 34° 22.40' N, 30° 2780' W. Depth 1,340 m. Collected by Serge Gofas, Bernard Métivier, and Anders Warén (1993–02–03). Repository: Muséum National d'Histoire Naturelle Paris.

Two specimens of *Micropilina arntzi* (Warén and Hain 1992) were studied in addition. Fixation 96% EtOH. Expedition name: R/V Polarstern ANT IX/3 1991, Station no. 180. Locality: Antarctica, Lazarev Sea, Coordinates 69° 57.5' S, 6° 20.0' E. Collected by Stefan Hain (1991 February 23). Depth 280–298 m. Repository: Swedish Museum of Natural History (SMNH), Type no. 4858.

Electron microscopy

Scanning electron microscopy (SEM) observation was carried out of both fractured specimens and of the shells' interiors. Samples were usually observed intact, although in some we removed the organic matter (with 5% NaOCl from 5 to 15 min). Samples were coated with carbon (Hitachi UHS evaporator) for variable pressure SEM (Leo 1430-VP) or field emission SEM (FESEM) observation (Leo Gemini 1530).

High-resolution transmission electron microscopy (TEM; Philips CM20) observations were carried out on both intact and in completely decalcified samples (2% ethylenediaminetetraacetic acid for several days). Samples were coated with carbon (Hitachi UHS evaporator).

Electron diffraction

The electron backscatter diffraction (EBSD) technique analyzes the diffraction pattern produced when backscattered electrons are diffracted by a crystalline material. This pattern, once indexed, provides information about the orientation of the crystal lattice and the space group of the crystal structure. Data from different positions can either be integrated into an orientation map or processed to represent pole figures in stereographic projection. Samples were

analyzed unpolished and only the organic matter was removed from the samples prior to analysis.

Two equipments were used: (1) EBSD detector TSL OIM 3.5 from EDAX Inc. coupled with a SEM Philips XL-30 (CITIUS, Universidad de Sevilla) and (2) Inca Crystal (Oxford Instruments) detector coupled to a Gemini-1530 (Carl Zeiss) FESEM (CSIRC, Universidad de Granada).

X-ray diffraction

For comparative purposes, additional samples of other molluscan classes have been analyzed with an X-ray diffractometer equipped with an area detector Bruker D8 Smart Apex (CSIRC, Universidad de Granada). The information obtained has been represented as pole figures with the specially designed software XRD2DScan.

Results

Morphology and arrangement of aragonite crystals

R. euglypta Towards the shell edges, crystals are very elongated, flat (~0.25-μm thick) plates of aragonite, which are much longer than they are wide (Fig. 1a). They are better described as laths, rather than tablets. Crystals may

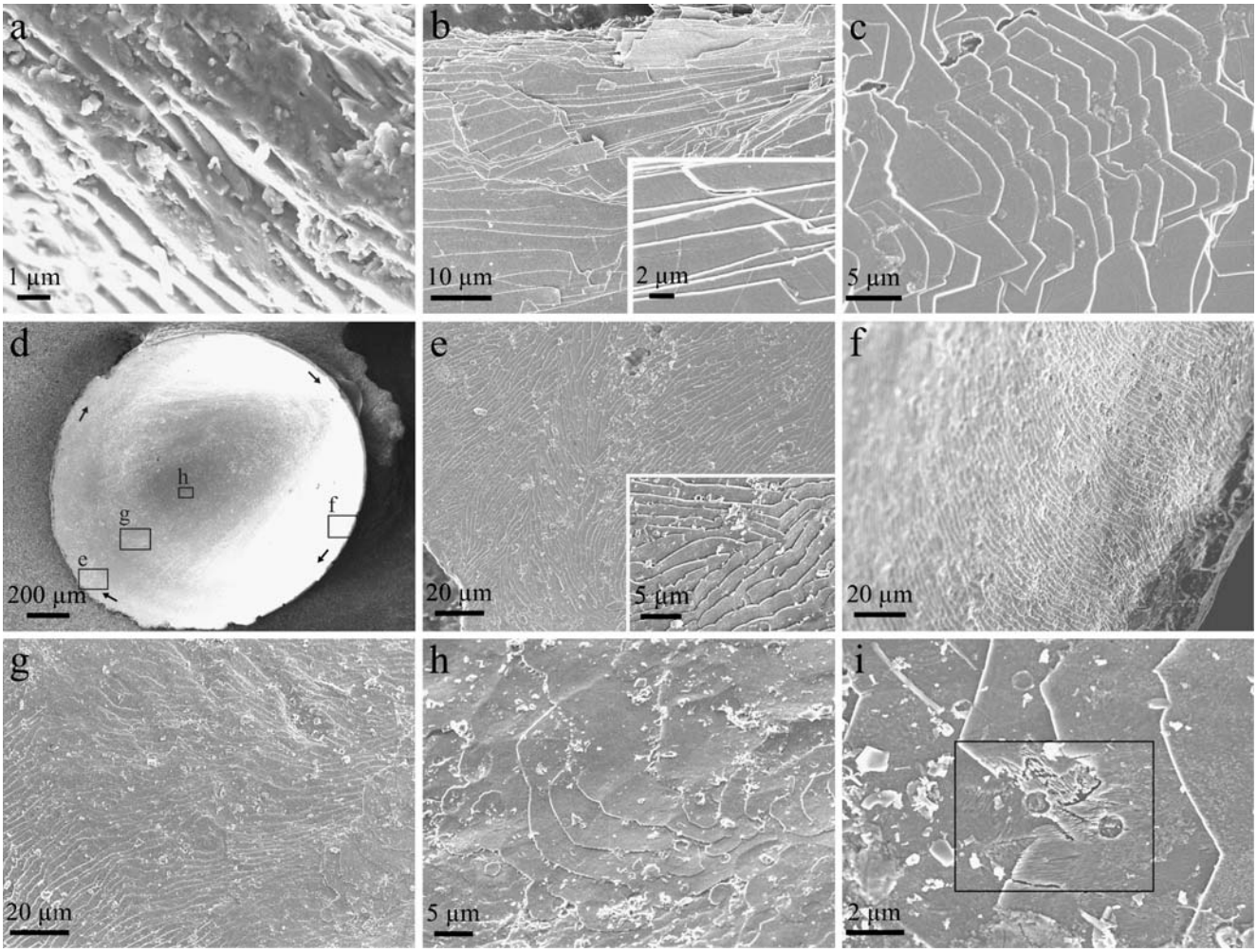

Fig. 1 *R. euglypta*. **a** Fracture view of the foliated aragonite; the internal shell surface is towards the bottom left. **b** Longitudinal fracture of the foliated aragonite to show the extension of laths; the *inset* shows a detail; the growth direction of lamellae is towards the left. **c**–**i** Views of the internal surface of the shell. **c** Surface view close to the posterior margin (*top*). **d** Whole view of one specimen, with indication of the areas corresponding to *e*, *f*, *g*, and *h*; the *small arrows* indicate the growth direction of the lamellae; the posterior area is towards the bottom left. **e** Posterior area; the lamellae grow parallel to the margin although their distribution is slightly dendritic; the *inset* shows how new lamellae intercalate between preexisting ones. **f** View of the left margin; lamellae grow parallel to the margin in a clockwise direction (compare to **e**). **g** Posterior area, towards the shell interior; lamellae change their orientation and are replaced by big tablets (visible to the right). **h** Detail of the plates growing in the central area of the shell. **i** Naturally corroded plates of the shell interior revealing their ultrastructure, which consists of oriented nanometric needles (particularly visible within the *square*); the changes in orientation of needles mark the boundaries between different crystals

attain lengths >100 μm (Fig. 1b) and their width varies between <1 and 12 μm (Fig. 1c). The growth fronts of individual laths change from arcuate to arrow-pointed (Figs. 1c,e and 4a). The crystals are coplanar and arrange into lamellae (Figs. 1c,e, f and 4a). All around the shell, the growth fronts of lamellae are quasiradial and slightly fingerprint like (Fig. 1e) and crystals grow parallel to the margin near the shell edge, in a sort of circumferential (clockwise) growth (Fig. 1d–f). Closer to the shell interior, the growth fronts of crystals become more sparse and change progressively into oblique (Fig. 1g). Closer to the center of the shell (i.e., at some 500 μm from the posterior edge), the latter arrangement is replaced (in fact, covered) by big flat plates with diameters of tens of micrometers (Fig. 1g–i). These are, in fact, radial aggregates of laths (Fig. 1h,i). Sometimes, several such plates can be seen growing concentrically (Fig. 1h). Rare spiral patterns are observed. When such plates are naturally corroded, an ultrastructure in the form of nanometric needles can be observed (Fig. 1i). The angle of divergence of needles in adjacent crystals was commonly found to be about 60° or 120°.

V. zografi The shell interior is covered by two different microstructures. A material identical to the one described for *Rokopella* is found covering the area extending from the apex to half the distance to the posterior margin (Fig. 2a). This material also extends from the posterior margin

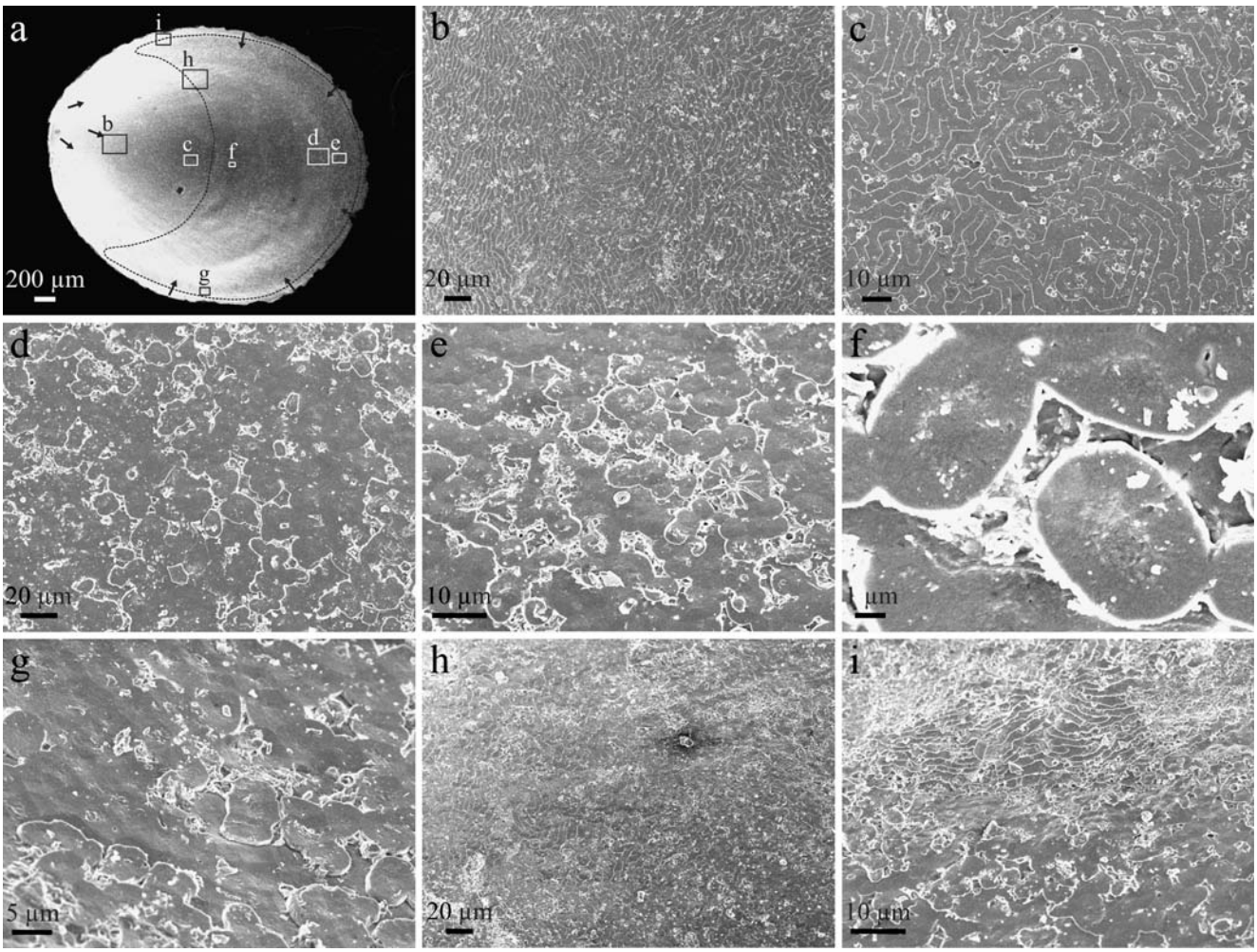

Fig. 2 *V. zografi*. **a** View of the interior of a complete specimen, with indication of the areas corresponding to *b*, *c*, *d*, *e*, *f*, *g*, *h*, and *i*; the *small arrows* indicate the growth direction of the lamellae of the foliated aragonite; the *broken line* delimitates the area occupied with nacre; the posterior area is towards the right. **b**, **c** Two views of the foliated aragonite secreted in the shell interior; there are frequent spiral growths, particularly in **c**. **d**, **e** Two views of the nacre secreted close to the posterior margin; growth fronts are diffuse and arranged step like. **f** Detail of nacre plates close to the shell center. **g** Slightly oblique view of the nacre close to the right margin. **h** Contact between nacre (*left*) and foliated aragonite (*right*) in an intermediate position between the shell center and the left margin. **i** Contact between foliated aragonite (*top*) and nacre (*bottom*) very close to the left margin

inwards to a distance of less than 100 μm in a specimen smaller than 3 mm in anteroposterior diameter (Fig. 2a). Lamellae grow towards the posterior side close to the apex and centripetally along the posterior edge (Fig. 2a,b,i). At the shell center, the growth patterns become chaotic, with some stacking plates sometimes displaying spiral growth and serving as centers for centrifugal growth (Fig. 2c), in a way very similar to that described for *Rokopella*. TEM observations on this material reveal that crystals are surrounded by organic membranes which are thicker than 100 nm. They appear electron transparent and homogeneous. Nacre is found in a continuous area which extends from close to the posterior margin to half the distance to the apex and depicted in Fig. 2a. It consists of typical nacre plates (between 5 and 8 μm in diameter and 0.5–0.7-μm thick) with oval slightly pseudohexagonal outlines (Fig. 2d–g), which sometimes merge together forming composite plates (Fig. 2d,e,g). The long dimension of plates may point in any direction. The growth fronts of nacre are step like, although slightly irregular, and grow centripetally close to the posterior margin, in concordance with those of the lamellae of aragonite laths (Fig. 2i). The transition between

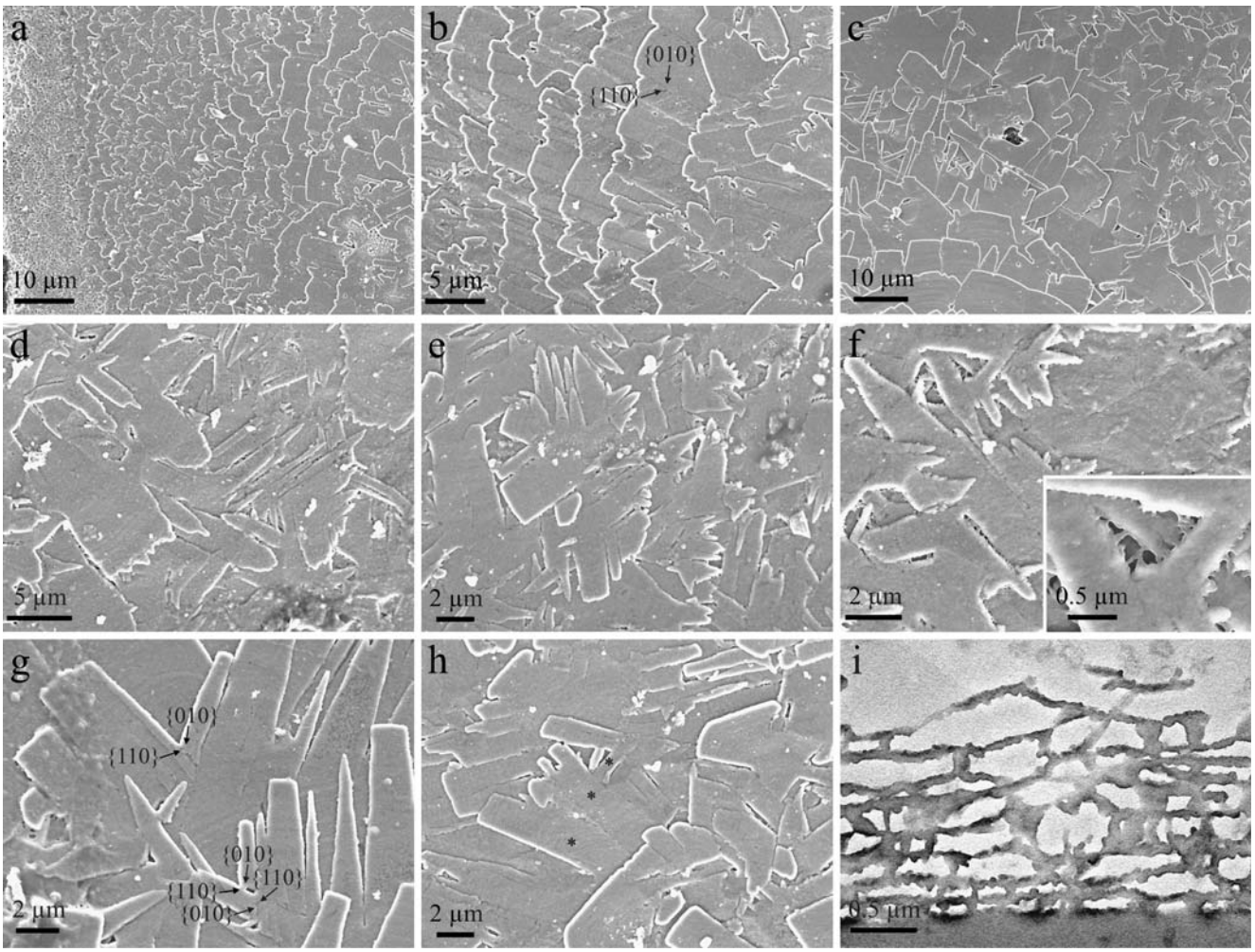

Fig. 3 *M. arntzi*. **a**–**h** Views of the internal shell surface; the posterior margin is always towards the left. **a** View of the posterior marginal area, to show the regularity of growth fronts; there is a general alignment perpendicular to the growth fronts. **b** Detail of the posterior marginal area; despite the general alignment, there are frequent crystal offshoots at 60°; some faces have been indexed to show the interfacial relationship between crystals. **c**–**h** Views of an area of the shell extending between 40 and 120 μm from the posterior margin in the direction to the apex, taken from the specimen in Fig. 5**a**. **c** The arrangement of crystals is extremely complex and the individual growth fronts of lamellae can hardly be traced. **d** Dendritic structure (*center*) composed of crystals branching at 60° from the central axis; crystals from different lamellae intercept each other (*top left*). **e** Area with frequent dendrites. **f** Crystals belonging to different lamellae interdigitate with each other; the *inset* shows the organic membranes surrounding crystals. **g** Detail to show the interfacial boundaries between crystals juxtaposing at 60°; some faces have been indexed with this goal. **h** Complex arrangement of crystals, with units separating at varied angles; some of them change their orientation during growth (*asterisks*). **i** Decalcified TEM section transversal to crystal elongation; the remaining organic membranes display an apparent brick wall arrangement

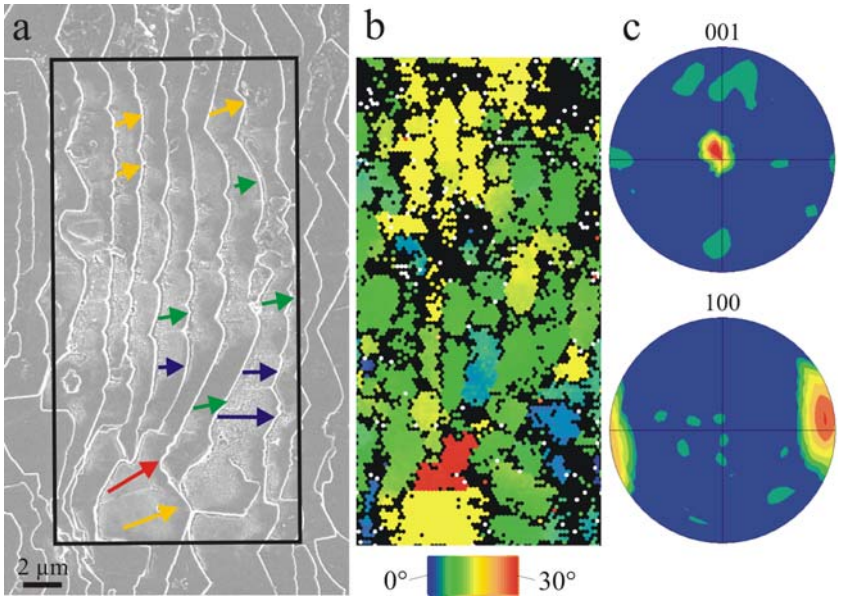

Fig. 4 EBSD map of an area corresponding to the posterior margin of a shell of *R. euglypta*. **a** Mapped area. **b** Orientation map of the *a*-axis; *colors* indicate the deviation of the *a*-axis relative to the horizontal from 0° to 30°; angles are constant within single crystals; the orientation of some selected crystals is given in **a** (*arrows*). **c** 001 and 100 pole figures; the 001 pole figure implies that the *c*-axis is slightly deviated from the vertical and the distribution of the 100 maxima implies that the *a*-axis is parallel to the growth direction of lamellae (compare to **a**)

the lathy material and the nacre is rather abrupt and takes place within a distance of about 10 µm (Fig. 2h,i).

M. arntzi All the internal surface is covered by a microstructure that is identical to the lathy lamellar material described in *Rokopella* and *Veleropilina*. The morphology of the laths observed agrees with the general descriptions provided above although the growth fronts of individual tablets are straight (Fig. 3a–h). Measured thicknesses are ~0.4 µm. The mean width of plates is around 3–4 µm, although extreme values range from <0.5 to >25 µm (Fig. 3a–d). Compared to the other two genera, the arrangement of crystals of *Micropilina* is very complex due to the fact that laths usually divide or juxtapose (Fig. 3b–h). Very frequently, there is a lath which constitutes the central branch and periodically emits other branches at some 60°, on either just one or both sides, in a semidendritic fashion (Fig. 3c–f). In some such instances in which the contacts between crystals are visible, it is clear that the side laths in fact juxtapose to the central lath (Fig. 3b,g,h). In rare instances, crystals meet or divide at lesser angles (~10°; Fig. 3h). In particular cases, the orientation of the crystals appears to change progressively (Fig. 3h). Towards the margin, the growth fronts of lamellae are comarginal and slightly oblique and are closely spaced to each other (Fig. 3a,b). This distance soon increases towards the shell interior (Fig. 3a,b). At the same time, the growth fronts become much more irregular (labyrinthine like) and obscure (Fig. 3c–e). This effect is enhanced by the complex relationships between crystals (Fig. 3c–h), which frequently intercept each other even if they pertain to different lamellae (Fig. 3c,d,f). TEM view of a decalcified sample reveals the existence of organic homogeneous membranes (60–70 nm thick) which surround the crystals (Fig. 3i). Similar organic envelopes are also visible under FESEM (Fig. 3f, inset).

EBSD analysis

R. euglypta A mapped 12×24-µm area close to the edge (Fig. 4a) provided coherent orientations for single tablets, which invariably have their *a*-axes parallel to their main elongations (Fig. 4a,b). The corresponding pole figures display discrete maxima (Fig. 4c). The 001 maximum is slightly offset (4–5°) from the center of the pole figure and the 100 poles are aligned with the growth direction of crystals. The approximate spread angle of the *a*-axis is 30°.

V. zografi No reliable data have been obtained on this species.

M. arntzi The different maps display similar results (Fig. 5a). As in *Rokopella*, the crystals display coherent orientations and elongate along the *a*-axis (Fig. 5b). Two large-sized maps, one close to the margin (30×40 µm) and the other at an intermediate position (20×30 µm), provided similar results (Fig. 5c,d). The 001 maximum is centered on the diagram and the 100 pole figures display a sixfold symmetry, in which one of the maxima is in the growth direction of lamellae. The map of a small area (20×9 µm), which includes a few tens of crystals, also shows the typical six-rayed symmetry of the 100 pole figures, but the maxima break into minor maxima, which are separated by some 10°

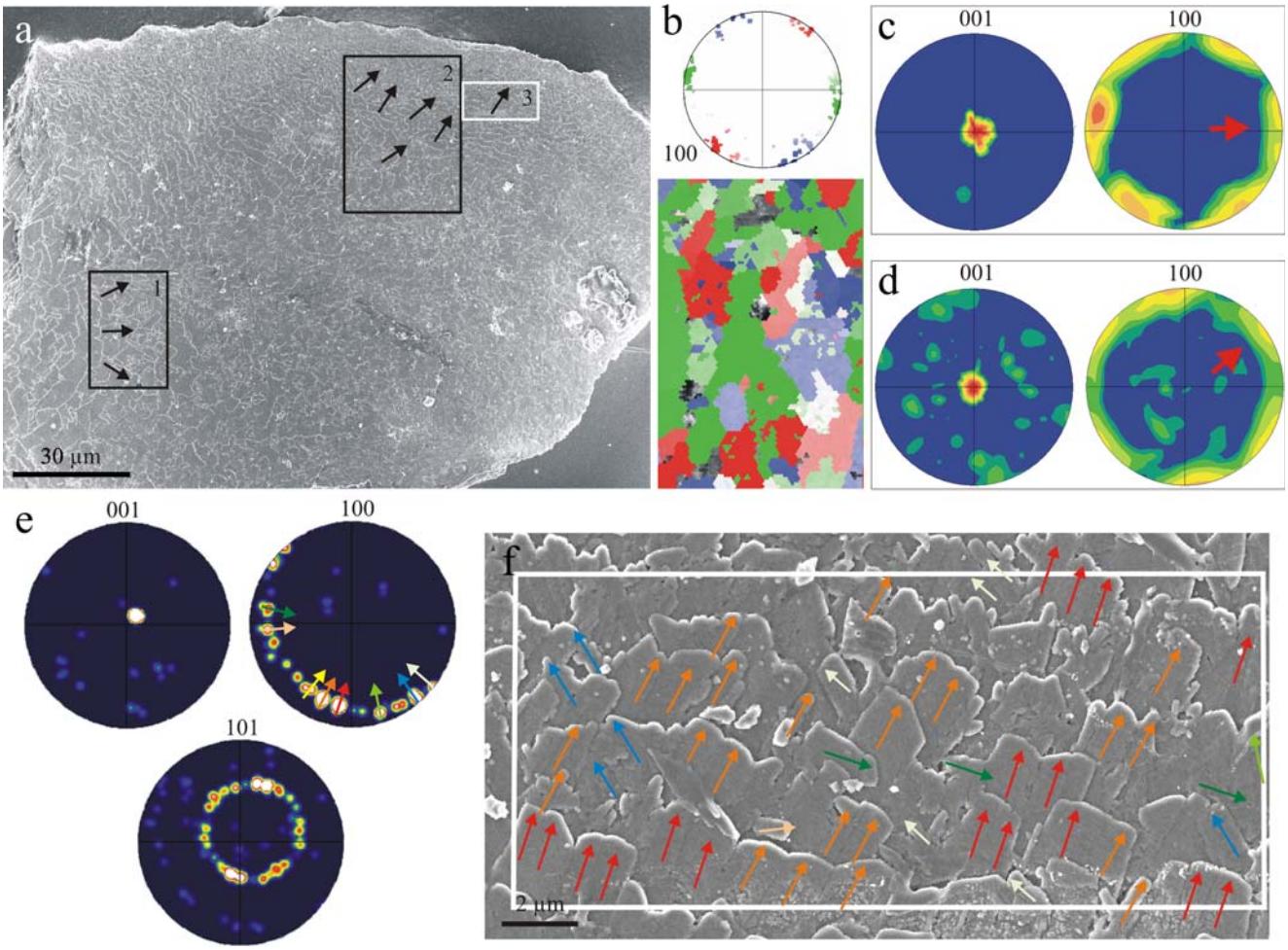

Fig. 5 EBSD maps on a shell fragment of *M. arntzi*. **a** General view of the fragment, with indication of the mapped areas and of the main growth orientations of lamellae (*arrows*); the posterior margin is towards the top. **b** 100 orientation map (*bottom*) and corresponding pole figure (*top*) of area *1*; orientation values come in *colors* and only the orientations in a range of 10° around the maxima have been represented in the pole figure; the orientation map implies that the crystals display coherent orientations and that divergence angles are about 60°. **c**, **d** 001 and 100 pole figures of the areas *1* and *2*, respectively; both 100 pole figures display a sixfold symmetry, with one of the maxima oriented in the mean growth direction of lamellae (*red arrowheads*); the scattering is greater in **c**, i.e., the area farther from the margin. **e** 001, 100, and 101 pole figures of area *3*; the 001 pole maximum implies that the *c*-axis is perpendicular to the surface of laths; the 100 pole figure displays a sixfold symmetry, which is even more evident in the 101 pole figure; each maximum is composed of several minor maxima separated by some 10°. **f** SEM view of area *3*; the orientations (*color arrows*) of the *a*-axis on selected crystals provided by the EBSD analysis have been plotted; the relationship of orientations to the minor maxima can be seen in the 100 pole figure of **e**; crystals on the same lamella may relate either at ~60° or ~10°

(Fig. 5e). Maps of this kind also reveal how adjacent crystals in the same lamella relate not only at 60° but also, though less frequently, at ~10° (Fig. 5f).

Discussion

The internal shell layers of monoplacophorans consist of two different microstructures: nacre (composed of tablets) and another lamellar (composed of laths) material, which has often been confused with nacre (see below). Nacre appears to be in the minority since it has only been identified in an area of the shell of *V. zografi* but not in the other two species examined. The implications of the recognition of both materials will be examined separately.

Morphology and crystallography of the foliated aragonite

This microstructure is basically composed of parallel aragonite laths, in which their main surfaces orient at a low angle (2–5°) to the shell surface. From the morphological viewpoint, the kind of aragonite crystals produced by monoplacophorans and their arrangement are unique among molluscs. Leaving aside the mineralogy, the described lathy lamellar material has a clear counterpart in

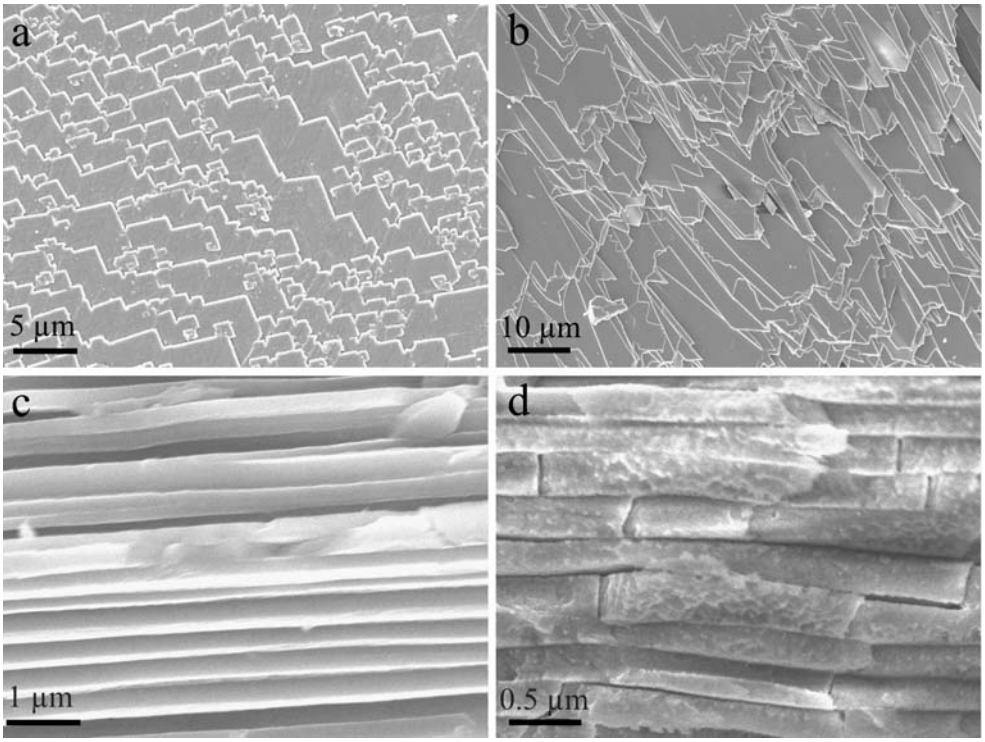

Fig. 6 Calcitic foliated layer of bivalves. **a** View of the internal shell surface of *Ostrea edulis*; the foliated layer is made up of oriented arrow-pointed laths, which arrange into lamellae; the growth direction is towards the upper right. **b** Surface view of the exfoliated shell of *Anomia ephippium*, showing the extent of laths; the growth direction is towards the bottom right. **c** Fracture view of the shell of *O. edulis* parallel to the elongation of laths, to show the lamellar aspect of the microstructure. **d** Fracture view of the shell of *A. ephippium* perpendicular to the elongation of laths; the aspect is brick wall like

the foliated layer, invariably calcitic, found in Pectinoidea, Ostreoidea, Anomioidea, and Limoidea (Bivalvia). The latter microstructure consists of thin (~0.4 μm) calcitic laths, with arrow-point endings that are arranged into lamellae or folia (Fig. 6). There is no crystallographic correspondence between the aragonitic and calcitic foliated microstructures since the main surfaces of the calcitic laths are $\{10\bar{1}8\}$ (Checa et al. 2007) and not {001} as in the foliated aragonite of monoplacophorans; nevertheless, in view of the morphological resemblance, we propose to apply the term foliated aragonite to this newly described monoplacophoran microstructure.

Our EBSD data imply that the individual laths are single crystals in which the *c*-axis is perpendicular to the main surface of the lath and the *a*-axis is invariably parallel to the main elongation (Figs. 4 and 5). Crystals display a common orientation of their *c*-axes independent of their position within the shell. With regard to the *a*- and *b*-axes there is a variable degree of alignment depending on the species and on the position on the shell. In *Rokopella*, pole figures obtained close to the edge indicate that the material is quite well ordered, with a maximum angle of divergence of the *a*–*b*-axes <30° (Fig. 4). We lack EBSD data of the internal tablets, but the observed nanoneedles forming the plates (Fig. 1i) are comparable to those found by Mutvei (1970, 1980, 1991) in the nacre of bivalves, gastropods, and *Nautilus*; we have found similar nanoneedles to be parallel to the *a*-axis in the bivalve *Pinctada margaritifera* (A. Checa, M. Rousseau, unpublished data). Therefore, the frequent angular relationships of 120° found between needles of adjacent crystals in *Rokopella* would strongly argue for polycyclic 110 twin relationships. Most likely, the same can be applied to the foliated aragonite of *Veleropilina*. Contrary to our findings, Chateigner et al. (2000) found that the *a*- and *b*-axes in the "nacre" of the monoplacophorans *N. galatheae* and *R. zografi* are completely disordered, probably because they used X-ray diffraction, which provides much poorer resolution than EBSD.

Ubukata (1994) and Checa and Rodríguez-Navarro (2001) stressed the importance of crystal selection by competition for an even alignment of crystal units. Competition can also occur in the marginal foliated aragonite of *Rokopella* and *Veleropilina*, where growth fronts are radial and centripetal, respectively, and crystals have a common growth direction, which produces an intense competition. Given the extreme elongation in the *a*-direction of the crystals used by monoplacophorans, competition imposes a final arrangement in which the *a*-axis is parallel to the growth direction of lamellae (Figs. 1c,e,f, 2b,i, and 4a). Towards the interior, where superimposed tablets are the dominant type of growth, crystals are free to diverge in any direction and twins dominate (Figs. 1g,h and 2c).

In *Micropilina*, the crystallographic arrangement of single plates is identical to that in *Rokopella*, but the relationships between plates are much more complex. Crystals very commonly diverge at 60° (Fig. 3a–h), although rarer divergences at ~10° (Figs. 3h and 5f) have also been observed. This is very much in agreement with the sixfold symmetry of EBSD pole figures. The spacing of

maxima at 60° fits in with the observed divergence angle of crystals (Fig. 5). When the contacts between crystals are evident, it is possible to observe how one of the {110} faces of the newborn crystals lean against the {010} face of its "parent" crystal (Fig. 3b,g). When only a few tens of crystals are mapped, each of the six big maxima of the pole figure is constituted by a cluster of smaller maxima at ~10°, i.e., in coincidence with the minor observed divergence angle (Fig. 5e,f). The commented angular and facial relationships are not known in inorganic aragonite, which is most likely due to the intervention of the organic fraction.

Despite the fact that EBSD maps of *Micropilina* include crystals belonging to many different lamellae, their associated pole figures consistently display a six-rayed symmetry. This suggests the process of epitaxy, in which new crystals nucleate onto previous crystals and inherit their orientation. This is also demonstrated by cases of coincidence in shape between laths of superimposing lamellae observed in the shells of *Rokopella* (Fig. 1c,h), *Veleropilina* (Fig. 2c), and *Micropilina* (Fig. 3b).

The growth fronts in *Micropilina* become subparallel close to the margin and much more irregular towards the interior (Fig. 3a–f). Although the frequency of crystal divergence persists, a greater degree of crystal order can be appreciated towards the margin, which fits in with the lesser scatter of the pole figure maxima of more marginal areas (compare Fig. 5c,d). As in *Rokopella*, crystal selection may also account for this increasing order.

The aragonitic foliated layer of monoplacophorans compared to molluscan nacre

Bivalve nacre tablets are essentially monocrystals, with extremely varied shapes (Wise 1970; Wada 1972; Checa and Rodríguez-Navarro 2005). As is always the case with nacre, crystals soon acquire their maximum height and later expand sideways until impinging on each other (Fig. S1a). The polygonal aspect of mature nacre is obtained this way (Fig. S1b). The growth fronts of nacre are arranged in a step-like formation with stacks of usually two or three, up to a maximum of six, growing crystals. Growth fronts can be defined as diffuse in the sense that they are formed by a pleyad of growing crystals, with the more advanced ones being in a more incipient stage of growth (Fig. S1a). Gastropod tablets are polygonal and are composed of many twinned crystals (Mutvei 1978), which stack in towers (Fig. S1c). Towards the bottom of the towers, crystals are in a more advanced growth stage, until the whole lamellar surface is tessellated (Fig. S1d). *Nautilus* nacre tablets are pseudohexagonal frequently twinned monocrystals (A. Checa, unpublished data). They stack in towers, in a gastropod-like fashion, close to the boundary with the outer fibrous layer (Fig. S1e). However, towards the interior, a bivalve-like mode of growth predominates (Fig. S1f). The shape and distribution of nacre tablets observed in the posterior area of *V. zografi* are fully comparable to those found in the mentioned groups (Fig. 2d–g). This nacre is particularly reminiscent of that found in bivalves, given the step-like distribution of growth fronts and their diffuse aspect.

In all cases, the shapes of nacre tablets are quite unlike those of laths composing the foliated layer of monoplacophorans. Nacre tablets have a maximum length to width ratio less than 2 and, accordingly, nacre is said to have a brick wall arrangement, independent of the direction in which it is cut. The length to width ratio of the laths composing the foliated aragonite of monoplacophorans has not been precisely measured but may easily go beyond 100. Therefore, this material can be said to have a pile of plank arrangement. It shows a brick wall arrangement when cut perpendicular to the main direction of laths (Fig. 3i) but a linear arrangement when cut parallel to the main elongation (Fig. 1b). This feature is also found in the calcitic foliated layer of bivalves (Fig. 6c,d).

As in nacre, the *c*-axis of aragonite laths of monoplacophorans is along the shortest dimension (compare 001 pole figures of Figs 4c and 5c,d to those of Fig. S2). But this is the only crystallographic similarity. In bivalves, it is the *b*-axis (and not the *a*-axis as in monoplacophorans) which is perpendicular to the growth fronts of lamellae (e.g., Wada 1960, 1961; Wise 1970; Weiner and Traub 1981; Checa and Rodríguez-Navarro 2001, 2005; Fig. S2a). The same applies to *Nautilus* nacre (A. Checa, A. Rodríguez-Navarro, unpublished results; Fig. S2b), although some authors have found a higher incidence of twins (Hedegaard and Wenk 1998; Chateigner et al. 2000). In Gastropoda, nacre crystals from adjacent towers have their *a*- and *b*-axes unevenly oriented (Wise 1970; Manne et al. 1994; Fig. S2c).

In addition, nacre displays other basic ultrastructural features. The nacre of molluscs is composed of lamellae of aragonite bricks separated by interlamellar organic layers. Each tablet is in turn surrounded by an intercrystalline organic membrane. Interlamellar membranes have a core of β-chitin fibrils sandwiched between two protein covers, whereas intercrystalline membranes consist of silk-fibroin (Levi-Kalisman et al. 2001). Cartwright and Checa (2007) revived the compartment hypothesis of Bevelander and Nakahara (1969) and Nakahara (1979), who showed that the interlamellar membranes form first and the tablets later grow in between them. All these studies show how interlamellar membranes in gastropods subtend between tablets of adjacent towers in a similar growth stage (Fig. S3a,b). During growth, a given tablet expands within the compartment formed between the membranes below and above it. In bivalves, the interlamellar membrane on top of a particular lamella of bricks extends for some distance beyond the

growth front at the same time that it approaches the interlamellar membrane at the bottom of the same lamella (Fig. S3c). In both bivalves and gastropods, the interlamellar membranes delineate compartments which constitute effective barriers that the crystals of a particular lamella cannot cross.

Meenakshi et al. (1970) distinguished between interlamellar and intercrystalline membranes in TEM sections of the decalcified "nacreous" layer of *Neopilina* (their Fig. 9) based solely on their horizontal and vertical distribution respectively, which is not a valid criterion based on the different nature of both kinds (see above). Additionally, these authors performed the chitosan test, which gave no evidence of chitin in *Neopilina*. This would imply that the main component of interlamellar membranes is absent, although we must keep in mind that this test is not fully reliable.

Besides the above-mentioned circumstantial evidence, there is a criterion which makes the existence of true interlamellar compartment-forming membranes in monoplacophorans unlikely. We have shown that, in *Micropilina*, crystals of different lamellae can easily interpenetrate (Fig. 3c,d,f). This behavior is never recorded in nacre because interlamellar membranes prevent crystals from going across different compartments (see above). Therefore, the preformed compartments provided by interlamellar membranes in nacre do not exist in monoplacophorans. A comparative overview of crystal and membrane distribution in bivalves, gastropods, and monoplacophorans is provided in Fig. 7.

The membranes found in the foliated aragonite of monoplacophorans (e.g., Fig. 3i) are rather comparable to the intercrystalline membranes described in nacre (see above) and in the foliated and fibrous calcitic microstructures (Watabe 1965; Travis and Gonsalves 1969). These are organic sheaths surrounding every crystal and expanding at the same time as the crystal.

Based on the absence of preformed interlamellar membranes, we can conclude that the foliated aragonite of monoplacophorans is a biomaterial which is completely separate from a true nacre. It is likely that the foliated aragonite is derived from nacre once this is deprived from its interlamellar membranes. This would inhibit the formation of compartments. On the other hand, the basic platy crystal (i.e., very short along the *c*-axis) of aragonite remains unaltered from one microstructure to the other. The fact that both microstructures appear intimately associated in the shell of *V. zografi* supports this hypothesis.

The transformation of brick-like crystals typical of aragonite into lathy ones of the foliated layer can also be explained within the context of the mineral bridge hypothesis of Schäffer et al. (1997), which implies that nacre plates of superimposed lamellae connect through the nanopores they observed upon decalcification of the intermediate interlamellar membranes of the gastropod *Haliotis*. Cartwright and Checa (2007) observed that the free not-yet-calcified interlamellar membranes of gastropods are also full of pores (up to 150 nm wide), whereas putative nanopores of bivalves are much more minute in size (~20 nm) and much less frequent. Cartwright and Checa (2007) hypothesized that the drastic differences in the size and frequency of nanopores in gastropods result in a much higher probability of nucleation of new crystals on top of others than in bivalves (Fig. 7a,b). Hence, gastropod nacre growth is tower like while bivalve nacre growth is terraced. Either in the presence of hypothetical interlamellar membranes completely deprived of nanopores or in the absence of such membranes, a growing crystal would not meet other growing crystals in a more advanced position. Accordingly, it would elongate uninterruptedly, thus acquiring the lathy aspect typical of foliated aragonite.

The issue of nacre in monoplacophorans

Foliated aragonite and nacre can be distinguished by the aspect of their growth fronts. These are sharp in the aragonitic foliated microstructure (Figs. 1c,e–i, 2b,c,h,i,

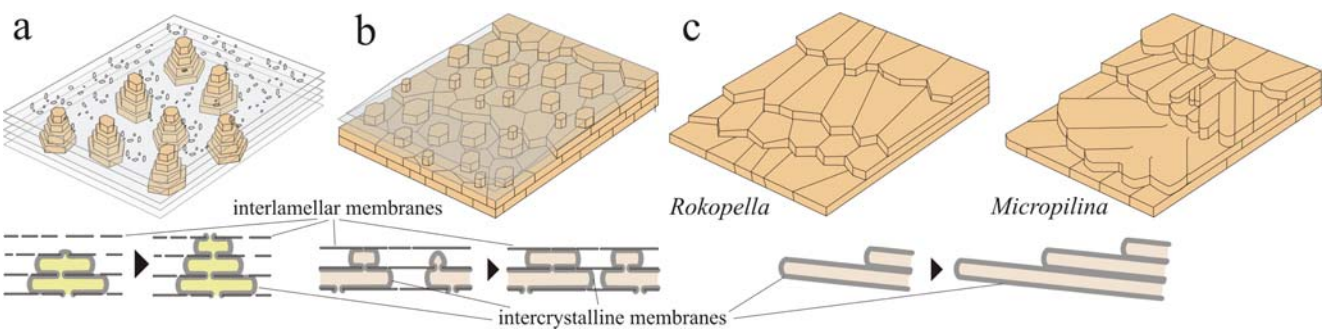

Fig. 7 Sketches reproducing the growth of nacre in gastropods (**a**) and bivalves (**b**), and of the foliated aragonite in monoplacophorans (**c**). **a** In gastropods, the frequent existence of nanopores in the interlamellar membranes causes nacre plates to stack in towers. **b** The infrequent existence of nanopores in bivalves causes predominant step-like horizontal growth. **c** Interlamellar membranes are absent in monoplacophorans and crystals grow uninterruptedly; the cases of marginal growth in *Rokopella* and *Micropilina* have been depicted

3a,b, 4a) and diffuse in nacre (Figs. 2d,e,g,i and S1a,c,e,f); at the same time, they are much more convolute (i.e., providing a more fingerprint-like general pattern) in the former.

Some earlier authors recognized nacre in monoplacophorans based solely on the brick wall appearance of the fractured or sectioned material (Schmidt 1959; Erben et al. 1968; Warén and Gofas 1996), which, as we discussed above, is an unreliable criterion. The only authors who provided photographs of the internal growth surface of the shell were Meenakshi et al (1970), Taviani et al. (1990), Cruz et al. (2003), and Urgorri et al. (2005). The photograph of a replica of the inner surface of *N. ewingi* (Meenakshi et al. 1970: Fig. 6) is so doubtful that the true nature of the microstructure shown cannot be discerned. The general appearance is similar to some areas of the foliated aragonite of *M. arntzi* (e.g., Fig. 3c). The photographs of the "nacre" of *Micropilina* sp. from the Pleistocene (Taviani et al. 1990: Fig. 1b) and *M. arntzi* (Cruz et al. 2003: Figs. 3 and 4) are undoubtedly of a typical aragonitic foliated layer, in concurrence with our observations on the same genus. Finally, Fig. 3e of Urgorri et al. (2005) was taken from the center of the internal shell surface of *Laevipilina cachuchensis* and also corresponds to an aragonitic foliated microstructure. This is also the case with the fractured "nacre" of *Laevipilina antarctica* in Warén and Hain (1992: Fig. 8).

In conclusion, previous studies do not yield conclusive evidence of nacre in monoplacophorans. Our finding of nacre in the shell of *Veleropilina* (Fig. 2d–g) is to date the first report of this iconic microstructure in the group and demonstrates that monoplacophorans share, even if marginally, this plesiomorphic molluscan trait. Future detailed observations in other living monoplacophoran taxa may contribute to expand the knowledge about the distribution of nacre and other microstructures within the group.

Evolutionary remarks

Our results imply that the internal nacreous layer is strongly reduced or absent and has been substituted by foliated aragonite in the studied species of Tryblidiida. The shell microstructure of the earliest Tryblidiida (possibly from the Middle Cambrian; Peel 1991) is unknown. Therefore, we do not know when the foliated aragonite appeared in the tryblidiidan lineage or whether it represents an ancestral condition for the group. This possibility fits in with the highly derived nature of tryblidiidans (Lindberg and Ponder 1996).

Runnegar (1983, 1985) figured the phosphate-replicated microstructure of the Lower Cambrian helcionelloid *Mellopegma georginensis*, consisting of evenly aligned rhombic plates. He correctly defined it as nacre and compared it to the nacre of bivalves. The same papers also referred to nacre in the helcionelloid *Anabarella* and in the earliest bivalves, all also from the Lower Cambrian. How early tryblidiidans relate to these early nacre-bearing groups is presently unknown.

Acknowledgements Serge Gofas (Departamento de Biología Animal, Universidad de Málaga), Anders Warén, and Karin Sindemark Kronestedt (Swedish Museum of Natural History) contributed in an essential manner by providing specimens. X-ray diffraction data of Fig. S2 are joint unpublished results of A.C. with Alejandro Rodríguez-Navarro (Departamento de Mineralogía y Petrología, Universidad de Granada). TEM sections of Fig. S3 are from the original material of the late Hiroshi Nakahara, kindly ceded by Mitsuo Kakei (School of Dentistry, Meikai University). J.R-R. is grateful to the Spanish Junta de Andalucía for his research grant. The study has been funded by Projects CGL2004-00802 and CGL2007-60549 (Ministerio de Educación y Ciencia) and by Research Group RMN190 (Junta de Andalucía).

References

Addadi L, Joester D, Nudelman F, Weiner S (2006) Mollusk shell formation: a source of new concepts for understanding biomineralization processes. Chem Eur J 12:980–987. doi:10.1002/chem.200500980

Bevelander G, Nakahara H (1969) An electron microscope study of the formation of the nacreous layer in the shell of certain bivalve molluscs. Calcif Tissue Res 3:84–92. doi:10.1007/BF02058648

Cartwright JHE, Checa AG (2007) The dynamics of nacre self-assembly. J R Soc Interface 4:491–504. doi:10.1098/rsif.2006.0188

Chateigner D, Hedegaard C, Wenk H-R (2000) Mollusc shell microstructures and crystallographic textures. J Struct Geol 22:1723–1735

Checa AG, Rodríguez-Navarro A (2001) Geometrical and crystallographic constraints determine the self-organization of shell microstructures in Unionidae (Bivalvia: Mollusca). Proc R Soc B 268:771–778. doi:10.1098/rspb.2000.1415

Checa AG, Rodríguez-Navarro A (2005) Self-organisation of nacre in the shells of Pterioida. Biomaterials 26:1071–1079 . doi:10.1016/j.biomaterials.2004.04.007

Checa AG, Esteban-Delgado FJ, Rodríguez-Navarro AB (2007) Crystallographic structure of the foliated calcite of bivalves. J Struct Biol 157:393–402. doi:10.1016/j.jsb.2006.09.005

Cruz R, Weismüller G, Farina M (2003) Microstructure of Monoplacophora (Mollusca) shell examined by low-voltage field emission scanning electron and atomic force microscopy. Scanning 25:12–18. doi:10.1002/sca.4950250104

Erben K (1972) Über die Bildung und das Wachstum von Perlmutt. Biomineral Res Rep 4:15–46

Erben HK, Flajs G, Siehl A (1968) Über die Schalenstruktur von Monoplacophoren. Akad Wiss Lit, Abh Math-Naturwiss Kl 1968:1–24

Hedegaard C, Wenk H-R (1998) Microstructure and texture patterns of molluscan shells. J Moll Stud 64:133–136. doi:10.1093/mollus/64.1.133

Lemche H, Wingstrand KG (1959) The anatomy of *Neopilina galatheae* Lemche, 1957. In: Bruun AF, Greve S, Spärck R, Wolff T (eds) Scientific results of the Danish deep-sea expedition round the world 1950–52, Galathea Report, volume 3. Danish Science Press, Copenhagen, pp 9–71

Levi-Kalisman Y, Falini G, Addadi L, Weiner S (2001) Structure of the nacreous organic matrix of a bivalve mollusc shell examined in the hydrated state using cryo-TEM. J Struct Biol 135:8–17. doi:10.1006/jsbi.2001.4372

Lindberg DR, Ponder WF (1996) An evolutionary tree for the mollusca: branches or roots? In: Taylor JD (ed) Origin and evolutionary radiation of the mollusca. Oxford University Press, Oxford, pp 67–75

Manne S, Zaremba CM, Giles R, Huggins L, Walters DA, Belcher A, Morse DE, Stucky GD, Didymus JM, Mann S, Hansma PK (1994) Atomic force microscopy of the nacreous layer in mollusk shells. Proc R Soc B 256:17–23

Meenakshi VR, Hare PE, Watabe N, Wilbur KM, Menzies RJ (1970) Ultrastructure, histochemistry, and amino acid composition of the shell of *Neopilina*. Anton Bruun Rep 2:3–12

Mutvei H (1970) Ultrastructure of the mineral and organic components of molluscan nacreous layers. Biomineral Res Rep 2:47–72

Mutvei H (1978) Ultrastructural characteristics of the nacre in some gastropods. Zool Scripta 7:287–296

Mutvei H (1980) The nacreous layer in molluscan shells. In: Omori M, Watabe N (eds) The mechanisms of biomineralization in animals and plants. Tokai University Press, Tokyo, pp 49–56

Mutvei H (1991) Using plasma-etching and proteolytic enzymes in studies of molluscan shell ultrastructure. In: Suga S, Nakahara H (eds) Mechanisms and phylogeny of mineralization in biological systems. Springer, Tokyo, pp 157–160

Nakahara H (1979) An electron microscope study of the growing surface of nacre in two gastropod species, *Turbo cornutus* and *Tegula pfeifferi*. Venus 38:205–211

Nakahara H (1991) Nacre formation in bivalve and gastropod molluscs. In: Suga S, Nakahara H (eds) Mechanisms and phylogeny of mineralization in biological systems. Springer, Tokyo, pp 343–350

Peel JS (1991) The Classes Tergomya and Helcionelloida, and early molluscan evolution. Bull Grønlands Geol Undersøgelse 161:11–65

Runnegar B (1983) Molluscan phylogeny revisited. Mem Assoc Australasian Palaeontol 1:121–144

Runnegar B (1985) Shell microstructures of Cambrian molluscs replicated by phosphate. Alcheringa 9:245–257

Schäffer TE, Ionescu-Zanetti C, Proksch R, Fritz M, Walters DA, Almquist N, Zaremba CM, Belcher AM, Smith BL, Stucky GD, Morse DE, Hansma PK (1997) Does abalone nacre form by heteroepitaxial nucleation or by growth through mineral bridges? Chem Mater 9:1731–1740. doi:10.1021/cm960429i

Schmidt WJ (1959) Bemerkungen zur Schalenstruktur von *Neopilina galatheae*. In: Bruun AF, Greve S, Spärck R, Wolff T (eds) Scientific results of the Danish deep-sea expedition round the world 1950–52, Galathea Report, volume 3. Danish Science Press, Copenhagen, pp 73–76

Taviani M, Sabelli B, Candini F (1990) A fossil Cenozoic monoplacophoran. Lethaia 23:213–216. doi:10.1111/j.1502-3931.1990.tb01361.x

Travis DF, Gonsalves M (1969) Comparative ultrastructure and organization of the prismatic region of two bivalves and its possible relation to the chemical mechanism of boring. Am Zool 9:635–661. doi:10.1093/icb/9.3.635

Ubukata T (1994) Architectural constraints on the morphogenesis of prismatic structure in Bivalvia. Palaeontology 37:241–261

Urgorri V, García-Álvarez O, Luque A (2005) *Laevipilina cachuchensis*, a new neopilinid (Mollusca, Tryblidia) from off North Spain. J Moll Stud 71:59–66. doi:10.1093/mollus/eyi008

Wada K (1960) Crystal growth of the inner shell surface of *Pinctada martensii* (Dunker) I. J Electron Microsc Tokyo 9:21–23

Wada K (1961) Crystal growth of molluscan shells. Bull Natl Pearl Res Lab Jpn 7:703–828

Wada K (1972) Nucleation and growth of aragonite crystals in the nacre of some bivalve molluscs. Biomineral Res Rep 4:141–159

Warén A, Gofas S (1996) A new species of Monoplacophora, redescription of the genera *Veleropilina* and *Rokopella*, and new information on three species of the class. Zool Scripta 25:215–232

Warén A, Hain S (1992) *Laevipilina antarctica* and *Micropilina arntzi*, two new monoplacophorans from the Antarctic. The Veliger 35:165–176

Watabe N (1965) Studies on shell formation. XI. Crystal-matrix relationships in the inner layers of mollusk shells. J Ultrastruct Res 12:351–370

Weiner S, Traub W (1981) Structural aspects of recognition and assembly. In: Balaban M, Sussman JL, Traub W, Yonath A (eds) Biological macromolecules. Balaban ISS, Philadelphia, pp 467–482

Wise SW (1970) Microarchitecture and mode of formation of nacre (mother of pearl) in pelecypods, gastropods and cephalopods. Eclogae Geol Helv 63:775–797